TÜBİTAK

Turkish Journal of Earth Sciences

http://journals.tubitak.gov.tr/earth/

Research Article

Turkish J Earth Sci
(2019) 28:

doi:10.3906/yer-1906-14

Source rock potential and depositional environment of the Lower Oligocene İhsaniye Formation in NW Turkey (Thrace, Karaburun)

Emilia TULAN[1,*], Reinhard F. SACHSENHOFER[1], Gabor TARI[2], Rachel FLECKER[3], Vanessa FAIRBANK[3], Magdalena PUPP[1], Ryan B. ICKERT[4]

[1]Montanuniversitaet Leoben, Leoben, Austria
[2]OMV Exploration & Production GmbH, Vienna, Austria
[3]School of Geographical Sciences, University of Bristol, Bristol, United Kingdom
[4]SUERC, Scottish Enterprise Technology Park, East Kilbride, Glasgow, United Kingdom

Received: 13.06.2019 • **Accepted/Published Online:** 07.08.2019 • **Final Version:** 00.00.2019

Abstract: The Lower Oligocene succession of the İhsaniye Formation, exposed at Karaburun on the Turkish (Thrace) coast of the Black Sea, provides insights into potential hydrocarbon source rock extent in the southwestern part of the Black Sea Basin. Presently, no detailed study of the İhsaniye Formation exists with regards to organic matter content and type. We analyzed 78 fine-grained samples from a c. 70-m-thick section near Karaburun. Relatively high total organic carbon (TOC) contents (average 1.45 wt.%) are present in the lower part of the İhsaniye Formation; the hydrogen index values reach a maximum of 252 mg HC/g TOC, indicating the presence of type III–II kerogen, and the organic matter is thermally immature (T_{max} 418 °C). The presence of foraminifera and TOC/S ratios below 2.8 confirm a fully marine environment. Elevated TOC contents and very low pristane/phytane ratios indicate an oxygen-depleted environment during deposition of the lower part of the İhsaniye Formation. The quartz/clay minerals ratio suggests a deepening trend in the lower part of the succession and a shallowing trend in the upper part. Peculiarly, the low salinity "Solenovian Event" (in nannofossil zone NP23) is not developed although Sr isotope ratios indicate that the basin was only connected to the Mediterranean for short periods during deposition of the İhsaniye Formation.

Key words: Paratethys, West Black Sea Basin, Lower Oligocene, hydrocarbon source rock, strontium isotopes

1. Introduction

The Black Sea is one of the last frontier petroleum basins in Europe. While reservoir presence and quality are generally considered the main exploration risk (e.g., Simmons et al., 2018), source rocks are widespread and have gained less attention. However, detailed investigations in recent years have shown that the petroleum potential of Oligocene ("Maikop-type") rocks in the Eastern Paratethys, including the Black Sea area, varies significantly and is partly limited (Pupp et al., 2018; Sachsenhofer et al., 2018a, 2018b). Hence, a more detailed examination of the hydrocarbon source potential of the Oligocene successions in the Black Sea region is advisable.

In the present study, Lower Oligocene rocks of the İhsaniye Formation, exposed near Karaburun (Thrace, NW of İstanbul) are investigated to expand regional knowledge of source rocks in the southwestern part of the Black Sea.

The Karaburun section is located in the West Black Sea Basin near the Çatalca gap, which formed a marine connection between the West Black Sea Basin and the Thrace Basin during Late Eocene and Early Oligocene time (Okay et al., 2019). The boundaries of the Çatalca gap are represented by the İstanbul Zone to the east and the Strandja Massif to the west (Figure 1).

The Cenozoic sediments in the Karaburun area include Upper Eocene shallow marine limestone of the Soğucak Formation (Less et al., 2011; Yücel et al., this volume) and the unconformably overlying (possibly latest Eocene to) Lower Oligocene İhsaniye Formation. The İhsaniye Formation is composed of sandstones, pelagic marls, and rare tuff horizons (Yurtsever and Çağlayan, 2002; Gedik et al., 2014). The biostratigraphy and the paleoenvironments of the İhsaniye Formation in the Karaburun section have been investigated in a companion paper by Simmons et al. (this volume).

The petroleum potential of the İhsaniye Formation has not previously been studied in detail, but regional-scale analogue data are available from age-equivalent Oligocene rocks in the West Black Sea offshore Bulgaria,

* Correspondence: emilia.tulan@gmail.com

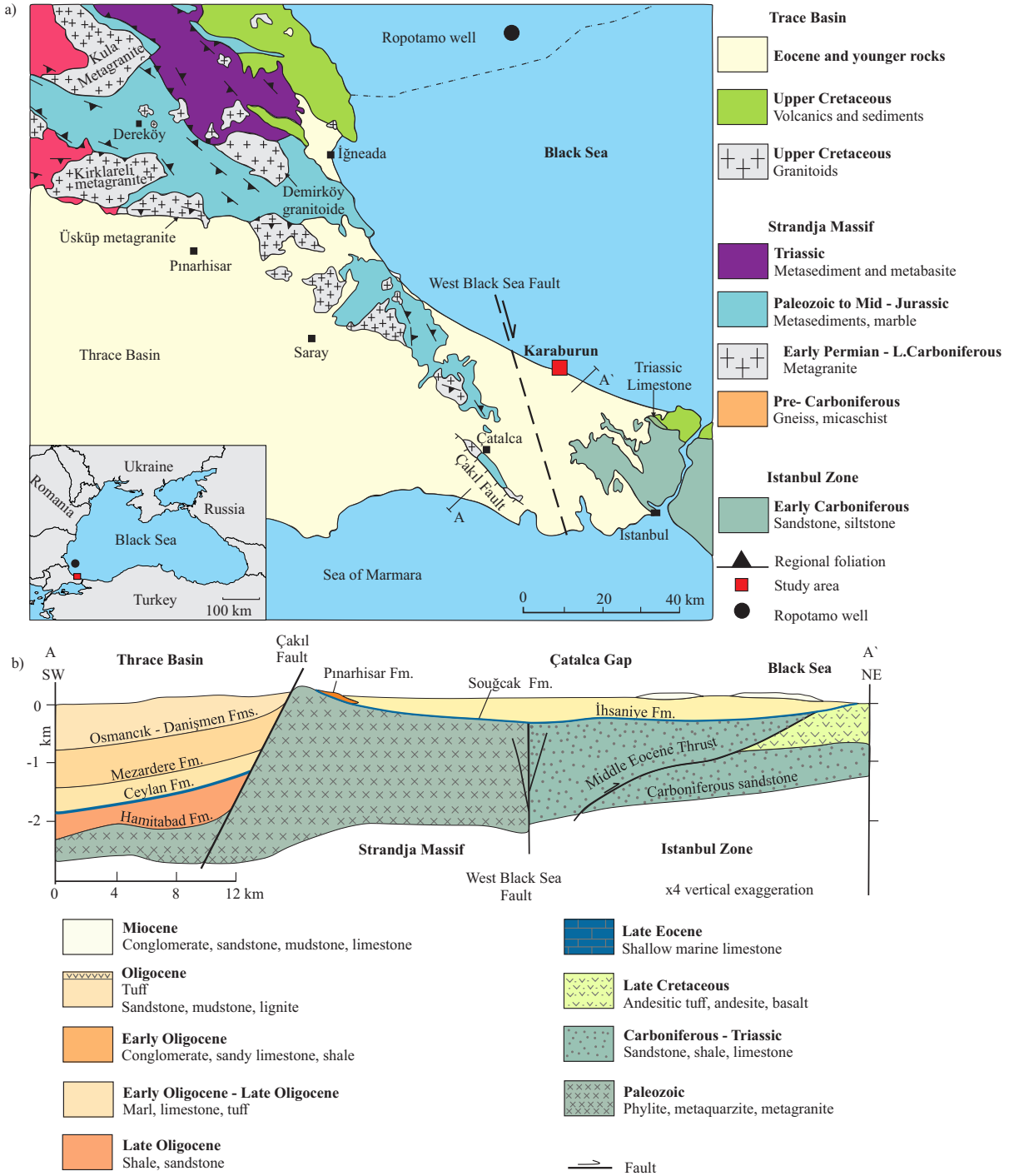

Figure 1. a) Geological map of the southern Strandja Massif and the neighboring regions (after Chatalov, 1988; Cheshitev and Kancev, 1989; Okay et al., 2001). b) Geological cross-section of the İhsaniye Formation (after Akartuna, 1953; Yurtsever and Çağlayan, 2002; Gedik et al., 2014, Okay et al., 2019).

where Sachsenhofer et al. (2009) and Mayer et al. (2018) showed that the Lower and Upper Oligocene successions hold a fair to good petroleum potential and, respectively, poor to fair from the Thrace Basin (Burkan, 1992; Sedat and Yalçın, 1997; Gürgey, 1999; Gürgey et al., 2003, 2005; Hoşgörmez et al., 2005; Huvaz et al., 2007; Gürgey and Batı, 2018).

At the beginning of nannoplankton zone NP23 (early Rupelian) the connection between the Paratethys and the world ocean was lost (Solenovian Event; Voronina and

Popov, 1984; Rusu, 1999); later it was partially restored in the upper NP23 (late Rupelian) (Popov et al., 1993). The evidence for the previously mentioned changes in connectivity is based on the paleontological data, documented in great detail by Popov et al. (2004).

Sachsenhofer et al. (2018a, 2018b) demonstrated that, across the region, source rock richness varies substantially during the late Eocene–early Oligocene and that this does not appear to be entirely coeval with episodes of connection or isolation. The aim of our study was to address this issue by quantifying the hydrocarbon source rock potential of the İhsaniye Formation in parallel with an independent assessment of the basin's connectivity history reconstructed using Sr isotopes as an isolation indicator (e.g., Flecker and Ellam, 2006).

2. Geological setting

The Karaburun section is located along the southwestern shoreline of the Black Sea, about 60 km northwest of İstanbul (Figure 1). A 15-km-wide marine gateway existed between the West Black Sea Basin and the Thrace Basin during the Late Eocene and Early Oligocene ("Çatalca gap"; Okay et al., 2019). The Eocene and Oligocene strata of the Çatalca gap conceal the West Black Sea Fault, a major Cretaceous strike-slip fault, separating the Strandja Massif and the İstanbul Zone (Okay et al., 1994). The Paleogene sequence consists of the Upper Eocene Soğucak Formation, overlain unconformably by the principally Lower Oligocene İhsaniye Formation and the Lower Oligocene Pınarhisar Formation.

The Soğucak Formation overlies the metamorphic rocks of the Strandja Massif in the west (Less et al., 2011), Carboniferous sandstones of the İstanbul Zone in the east, and probably Upper Cretaceous volcanic rocks in the north along the Black Sea coast (Okay et al., 2019). The Soğucak Formation is composed of thickly bedded to massive, light gray shallow-marine limestones, 5- to 60-m thick. The limestone contains corals, bivalves, algae, bryozoans, and larger benthic foraminifera (Less et al., 2011; Yücel et al., this volume). The top of the Soğucak Formation is formed by a major erosional unconformity.

Deposition of the İhsaniye Formation commenced during the latest Eocene (Late Priabonian) in the center of the Çatalca gap but only expanded to marginal areas including the Karaburun area in the Early Oligocene (e.g., Okay et al., 2019; Simmons et al., this volume; Figure 1). It is composed of open marine marls with a rich microfauna and microflora of foraminifera, calcareous nannofossils, and dinoflagellates; calcarenite; acidic tuffs; and rare pebbly sandstone beds (Okay et al., 2019; Simmons et al., this volume). The lower Oligocene Pınarhisar Formation (e.g., Popov et al., 2004; İslamoğlu et al., 2010), a brackish to lagoonal sequence with sandy limestone and shale, interfingers with the İhsaniye Formation near the Çatalca ridge.

The Karaburun area is one of the few localities in Turkey where Eocene and Oligocene formations are exposed along the Black Sea coast. Several authors have described the stratigraphy of the Karaburun area and attributed a Lower Oligocene age to the İhsaniye Formation (Oktay et al., 1992; Sakınç, 1994; Less et al., 2011; Gedik et al., 2014; Natal'in and Say, 2015; Okay et al., 2019; Sancay and Batı, this volume).

Based on the investigation of calcareous nannoplankton, foraminifera, and palynomorphs, Simmons et al. (this volume) recognized that the sediments of the İhsaniye Formation are no older than 33.9 Ma (nannoplankton zone upper NP21) and no younger than 31 Ma (lower NP23). They also presented a revised tectonic interpretation in which the deposition of the İhsaniye Formation was controlled by a now inverted normal fault. The following description of the İhsaniye Formation follows these authors. Sediments ranging in age from nannoplankton zone upper NP21 to lower NP23 were deposited on the hanging wall side of the fault ("Hanging Wall Section", Figure 2), whereas deposition on the footwall commenced only during NP23 ("Footwall Section", Figure 2).

The Hanging Wall Section is in its lower part (c. 40-m thick) dominated by marls with carbonate-rich siltstone or fine sandstone and minor debris flow horizons. In the upper part of the section, about 30-m thick, debris flow deposits' syn-sedimentary faults become increasingly significant. Debris flow deposits contain blocks of the Soğucak Formation, more than 1 m in size. Debris flows in the upper part of the Hanging Wall Section contain, in addition, volcanic rocks reworked from the underlying Late Cretaceous succession. Simmons et al. (this volume) suggested that deposition of the marl-dominated facies occurred in outer shelf to upper bathyal environments.

The Footwall Section includes two parts. The lower 15 m of the Footwall Section are represented by mixed pebbly calcareous sandstones, siltstones, and calcarenites with rare thin marl layers deposited in a fan-delta to shoreface environment. The upper part of the Footwall Section is formed by a 30-m succession of gray marls with thin calcareous siltstone layers, similar to those from the Hanging Wall Section.

3. Samples and methods

In total, 78 marl samples from the İhsaniye Formation were collected west of Karaburun along the Black Sea coast (Figure 2). Samples 1 to 70 were from the Hanging Wall Section, whereas samples 71 to 78 were taken from the marly upper part of the Footwall Section (Figure 2).

Their bulk mineralogical composition was determined with a Bruker AXS D8 Advance X-ray diffraction

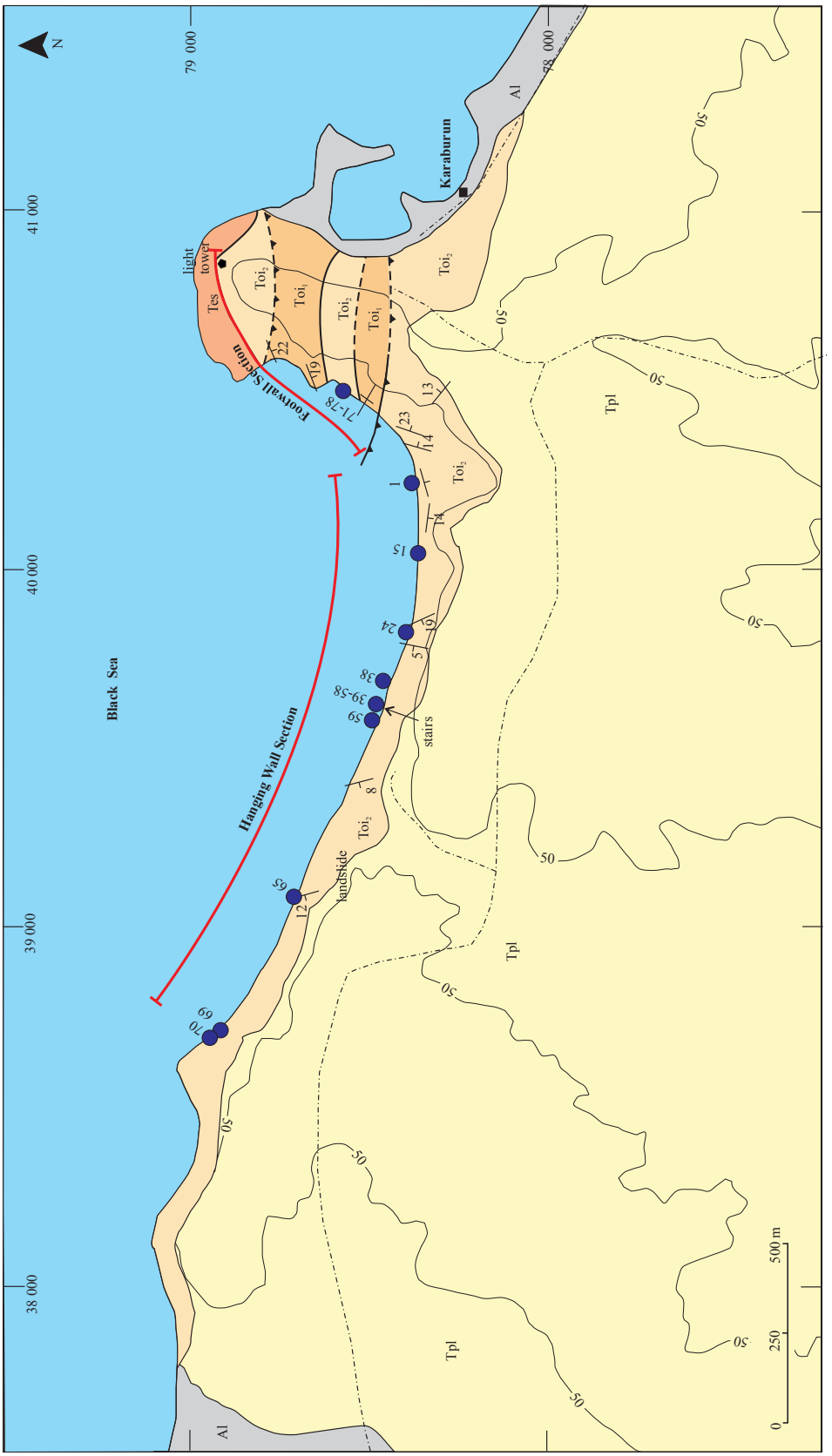

Figure 2. Geological map of Karaburun area (after Okay et al., 2019; Simmons et al., this volume) with the position of the samples collected for this study.

spectrometer (copper radiation generated at 40 kV and 40 mA). The powdered samples were placed carefully in sample holders to create a flat upper surface to achieve a random distribution of lattice orientation. To identify and quantify the different mineral phases, the software Diffrac. Eva and the method described by Schultz (1964), which is based on peak heights, were used.

Total carbon (TC), total sulfur (S), and total organic carbon (TOC) contents were analyzed using an ELTRA Elemental Analyzer for all 78 samples. Samples for TOC measurements were decarbonized with concentrated phosphoric acid. Results are given in weight percent (wt.%). Total inorganic carbon (TIC) was determined (TIC = TC – TOC) and used to calculate calcite equivalent percentages (TIC × 8.333).

Pyrolysis measurements were performed using a "Rock-Eval 6" instrument. The amount of free S1 hydrocarbons (mg HC/g rock) and the amount of S2 hydrocarbons generated during pyrolysis (mg HC/g rock) were determined and used to calculate the petroleum potential (S1 + S2 [mg HC/g rock]), the production index (PI = S1/(S1 + S2) (Lafargue et al., 1998)), and the hydrogen index (HI = S2/TOC × 100 [mg HC/g TOC]). Tmax was measured as a maturity indicator.

Polished blocks were prepared for ten samples. Semiquantitative maceral analysis using reflected white light and fluorescence light and vitrinite reflectance measurements were performed using an incident light Leitz microscope and following established procedures (Taylor et al., 1998).

Thin sections were prepared from 17 samples. They were studied using a Leica DM 2500P microscope and pictures were taken with a Leica DFC490 camera.

Eleven samples were selected for biomarker analysis and extracted using dichloromethane in a Dionex ASE 200 accelerated solvent extractor at 75 °C and 50 bar. Afterwards, asphaltenes were precipitated with a hexane/dichloromethane solution (ratio 80:1 according to volume) and separated by centrifugation. Medium-pressure liquid chromatography (MPLC) using a Köhnen-Willsch instrument was used to separate the hexane-soluble fractions into NSO compounds, saturated hydrocarbons, and aromatic hydrocarbons (Radke et al., 1980).

The saturated and aromatic hydrocarbon fractions were analyzed by a gas chromatograph equipped with a 30-m DB-5MS fused silica column (i.e. 0.25 mm; 0.25-mm film thickness), coupled to a ThermoFisher ISQ Dual-quadrupole mass spectrometer. Using helium as a carrier gas, the oven temperature was programmed from 70 °C to 300 °C at 4 °C/min increase, followed by an isothermal period of 15 min. With the injector temperature at 275 °C, the samples were injected seamlessly. The spectrometer was operated in electron ionization mode over a scan range from m/z 50 to 650 at 0.7 s total scan time. The data were processed with an Xcalibur data system. Individual compounds were identified by retention time in the total ion current chromatogram and comparison of the mass spectra with published data. Percentages and absolute concentrations of various compound groups in the saturated and aromatic hydrocarbon fractions were calculated using peak areas in the gas chromatograms and their relations to the internal standards (deuterated n-tetracosane and 1,1′-binaphthyl, respectively). Concentrations were normalized to TOC.

For strontium isotope analysis, foraminifera were separated from semiconsolidated sediment samples by covering with water in a plastic bottle and agitating until the sample disaggregated. This material was dried and sieved, and planktic foraminiferal tests were picked by hand under a binocular microscope. After picking, samples were cleaned using the clay removal technique described by Barker et al. (2003), in which the picked foraminifera were lightly crushed and then agitated in water to flocculate and decant residual clay. Carbonate samples were weighed into PFA vials and leached in ammonium acetate to remove groundwater salts and displace contaminant Sr on exchangeable sites (e.g., Bailey et al., 2000). The remaining material was rinsed twice in deionized water and then dissolved in dilute HCl. All HCl and HNO_3 were prepared by subboiling distillation in PFA (e.g., Mattinson, 1972). Sr was separated from matrix elements using Sr.Spec resin (Horwitz et al., 1991, 1992) using a nitric acid chemistry procedure adapted from Pin et al. (1994), in which samples are loaded in 8 M HNO_3, cleaned in sequential steps of 8 M HNO_3 and 3 M HNO_3, and Sr eluted in 0.01 M HNO_3. After ion exchange chemistry, samples were loaded onto purified Re filaments in a Ta emitter solution (cf., Birck, 1986). Total procedural blanks yielded values ranging from 300 to 500 pg, which are negligible relative to the amount of sample run. Isotopic analyses were conducted on a VG-Sector-54 thermal ionization mass spectrometer using a three-cycle dynamic multicollector routine and an exponential mass fractionation correction relative to $^{86}Sr/^{88}Sr = 0.1194$ (e.g., Nier, 1938; Steiger and Jager, 1977; Moore et al., 1982; Hans et al., 2013). Filaments were slowly heated to 2.4 A, and then focusing and filament current was adjusted to achieve a stable 10^{-11} A ion beam on ^{88}Sr. Analyses were typically run for 15–20 blocks of 10 cycles for approximately 1.5–2 h. Rubidium interferences were monitored but were negligible. Typical precision on the $^{87}Sr/^{86}Sr$ is ±20–30 ppm (2SE). Repeated measurements of reference material NBS987 at similar run conditions (0.5–1.5 × 10–11 A) during the period over which these analyses were conducted yielded a value of 0.710259 (±0.000027 2SD; n = 68), within uncertainty of the convention value of 0.71025, and indicates that the measurement repeatability is commensurate with the within-run uncertainty.

4. Results

The results of the analytical work carried out on 78 samples are presented below focusing on lithology, geochemical characteristics, biomarkers, and strontium isotope ratios.

4.1. Lithology

Two profiles within the İhsaniye Formation were investigated: the Hanging Wall Section and a part of the Footwall Section. Both of the sections are separated by a major fault normal fault (now an inverted fault, see Figure 2). To the west of the major fault is located the Hanging Wall and to the east/north the Footwall Sections. The Hanging Wall Section includes sediments approximately 70-m thick and is represented by samples 1 to 70. The section is well exposed (Figure 3) and only small parts are covered by vegetation or landslides. Nonexposed parts are marked by question marks in Figure 4. The studied composite section is represented by the alternation of light gray marl, carbonate-rich siltstone, and sandstone as well as tuffaceous beds between 56.8 and 58.0 m (Figure 4). The frequency of the siltstone layers generally decreases gradually upwards (Figure 3), but a few meters above the tuff level there is a gradual change from an

Figure 3. a–d: Studied outcrop of the Hanging Wall Section of the İhsaniye Formation with detail pictures (selected sample locations are shown for reference). a, b) Lower part of the section represented by organic-rich marls intercalated with calcareous sandstones. c) upper part of the section represented by organic-free marls with fewer calcareous sandstone layers; d) top of the studied section covered by the debris flow.

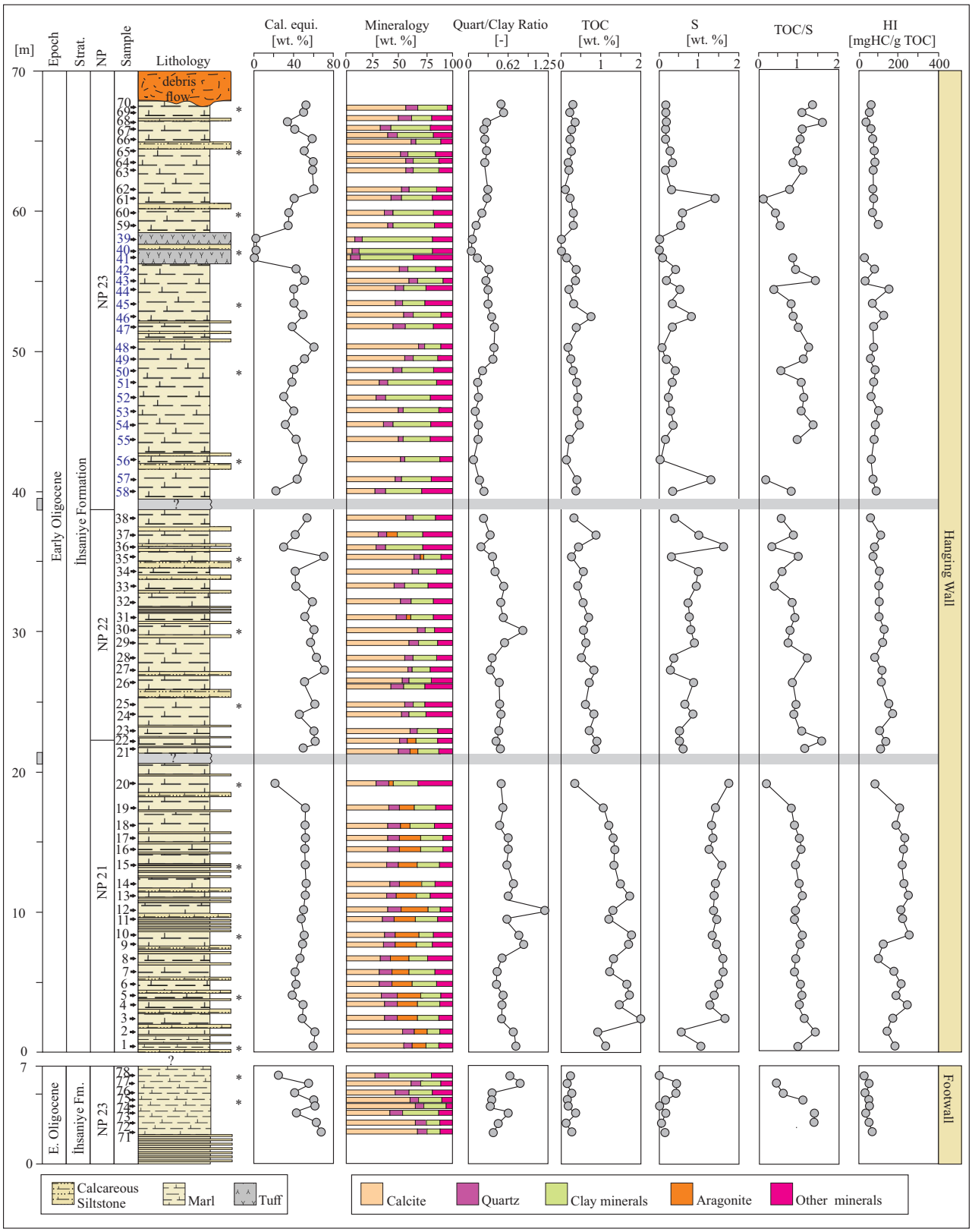

Figure 4. Bulk geochemical parameters and mineralogy of the İhsaniye Formation. Cal. equi. - calcite equivalent; TOC - total organic carbon; S - total sulfur; HI - hydrogen index; other minerals: pyrite, feldspar, ankerite, siderite, dolomite. * position of thin sections.

argillaceous marlstone to a sandy marlstone (Figure 4) displaying a coarsening upwards trend. At about 68 m, the fine-grained sediments are overlain by a prominent mass transport deposit that has a channelized geometry and includes reworked Eocene limestones clasts from the underlying Soğucak Formation and Cretaceous volcanic and metamorphic clasts.

Marls are dark gray when freshly broken, compact, and often contain macroscopically visible bioclasts (~2 mm), mostly foraminifera. Laminations are not visible, presumably because of complete bioturbation. Bioturbation structures are visible in a single sample (at 4.9 m of Hanging Wall Section). Under the microscope, the marls consist of a (micro-) sparitic to micritic matrix (Figure 5) with frequent foraminifera tests and a variety of detrital grains. A detailed microscopic description of the samples is given in Table 1.

Siltstones and sandstones consist of carbonate and lithic grains and abundant bioclast components (Okay et al., 2019). In thin sections, the calcareous sandstones are dominated by a variety of bioclast: cryptostome bryozoan, echinoderm debris, coralline algae, coral fragments, mollusk debris, and small indeterminate foraminifera (Figure 5). Angular quartz and lithic fragments are rare, although volcaniclastic fragments are present. Many clasts observed in the calcareous sandstone are reworked from the overlying Soğucak Formation and volcaniclastic basement, as well as the contemporaneous shelf.

Tuffaceous rocks are fine-grained and homogeneous. They have a light gray to whitish color and are very compact and much harder than the surrounding rocks. The microscopic observation reveals the presence of altered glass with an intersertal texture (Figure 5).

In thin sections, the organic matter is more abundant in the lower part of the Hanging Wall Section (0.5–19.1 m), compared to the remaining part of the section and the Footwall Section, where organic matter is rare and frequently replaced by pyrite.

Selected XRD diffractograms are presented in Figure 6. According to the XRD analysis, the major mineral constituents of the samples are calcite (48%) and clay minerals (24%), whereas quartz, feldspars, pyrite, ankerite, siderite, and dolomite occur as minor constituents (Figure 4). Aragonite occurs in significant amounts in the lower part of the Hanging Wall Section, and a single sample from the same section (46.9 m) contains gypsum (4%).

Based on mineralogy, the Hanging Wall Section can be subdivided into a lower part (0–19 m; samples 1–19) and an upper part (21.9–67.5 m; samples 20–70). The lower part is characterized by abundant aragonite (avg.: 18%) and, except for the lowermost samples, relatively uniform calcite (~40%) and quartz contents (~10%).

The upper part of the Hanging Wall Section is characterized by stronger compositional variations, and aragonite is present (in minor amounts) only below 36.9 m (samples 20–37; avg.: 3%). Samples from the tuff layer (56.8–58.0 m) are characterized by very high percentages of montmorillonite (avg.: 62%), which was formed by the alteration of volcanic glass (Figure 6). High percentages of clay minerals are also observed in mudstones between 42.2 and 47.8 m (samples 56–51), an interval that contains low amounts of detrital quartz (3%–9%). Consequently, the clay minerals/quartz ratio of these samples is very low (~0.1). Interestingly, there is a general upward decrease in the clay minerals/quartz ratio, which starts in the lower part of the section (sample 9 at 7.9 m) and terminates in the middle part of the upper part (sample 56 at 42.2 m) (Figure 4).

The Footwall Section is represented by pebbly sandstones and marls that onlap on the limestone of the Soğucak Formation. Although the marly part of the Footwall Section is up to 30-m thick (Simmons et al., this volume), we study only 7 m of this succession (samples 71–78 in Figures 2 and 4). In thin sections, the samples are characterized as fossiliferous sandy marlstones (Table 1). In the fine-grained part of the Footwall Section, the content of calcite minerals decreases upwards, whereas clay minerals increase in the same direction (Figure 4).

4.2. Bulk geochemical parameters and organic petrography

Bulk parameters of the İhsaniye Formation are plotted versus vertical section position in Figure 4 and are listed in the appendix. The bulk parameters of the Hanging Wall Section support the subdivision into a lower (samples 1–19) and an upper part. The lower part is relatively rich in TOC (1.0%–2.04%; avg.: 1.45%). In contrast, the upper part (samples 20–70) has an average TOC of 0.38 wt.%. Within the upper part, the TOC contents decrease from 0.9% at 23.0 m (sample 23) to 0.2% at 62.2 m (sample 56). Above this height, the TOC content remains low (avg.: 0.3%). Unsurprisingly, the tuff layer is largely free of organic matter.

Sulfur contents typically follow the TOC trend, but a few organic-lean samples from the upper part of the succession contain high sulfur contents. TOC/S ratios are 2.0 and show upward decreasing trends between samples 21 (21.9 m) and 57 (40.8 m) and between 56 (42.2 m) and 61 (60.9 m). Moreover, an increasing upward trend is seen between 61 (60.9 m) and 70 (67.5 m).

S2 values reach a maximum of 4.48 mg HC/g rock (Figure 7) and HI values in the lower part of the succession vary between 140 and 252 mg HC/g TOC, indicating the presence of type III–II kerogen, whereas HI values in the rest of the section (23–162 mg HC/g TOC) classify the organic matter as type III kerogen. A plot of HI versus Tmax (Figure 7) shows that the organic matter is immature.

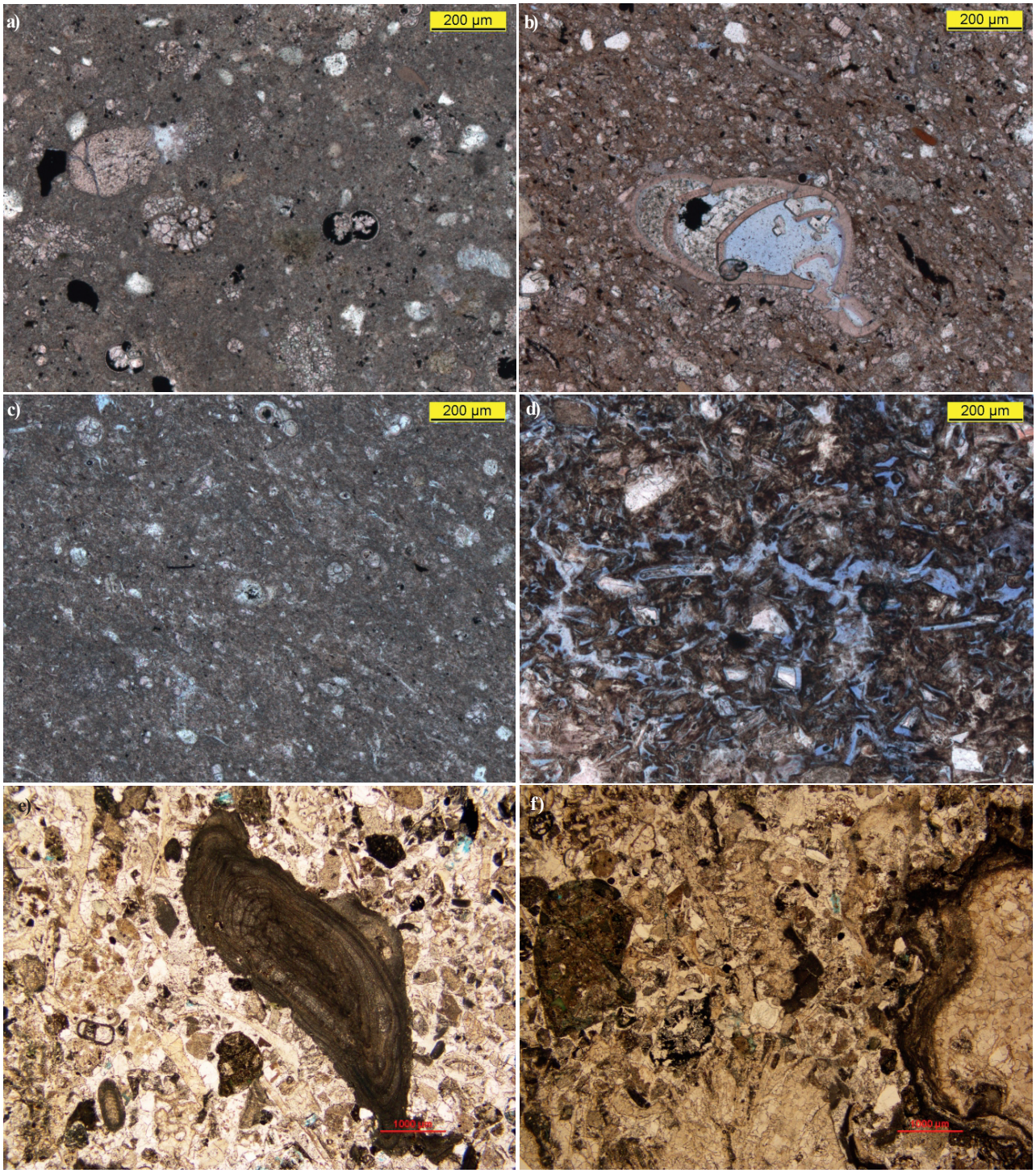

Figure 5. Thin section photographs. Footwall Section: a) Sample 75 (4.8 m) - Fossiliferous sandy marlstone with a matrix composed of micrite; Hanging Wall Section: b) Sample 1 (0.5 m) - Silty marlstone with a matrix composed of microsparite with few intraclasts and fossils; c) Sample 56 (42.2 m) - Marlstone with a matrix composed by microsparite and micrite with frequent foraminifera; d) Sample 40 (57.1 m) - Tuff consisting of altered volcanic glass with an intersertal texture; Calcareous sandstone (photographs courtesy of Mike Simmons): e) Sample below 35 (34.8 m): bioclastic grainstone with a variety of fragmentary bioclasts: coralline algae (centre of image), mollusk debris and small indeterminate foraminifera; f) Sample below 66 (64.7 m) bioclastic grainstone with coral fragments some with algal or cyanobacterial encrustations.

Table 1. Thin section descriptions.

Lithotype	Description	Env.	No.	
Argillaceous to sandy marlstone	Sandy marlstone with a micrite matrix; detritus grains (C), moderately sorted: feldspars (pl. (15–33 μm) and ksp. (21–58 μm)), some of the feldspar. Are altered by chlorite or sericite, and few present inclusions; few subrounded to rounded quartz (11–45 μm); biotite; glauconite. Fossils (C): globigerinid in intact condition; some are filled with framboidal pyrite.	basin	65,70	Hanging Wall Section
	Argillaceous marlstone; detritus grains (R): rounded quartz (5-13 μm), ksp. (39 μm) covered with sericite; framboidal pyrite. Fossils (F): planktonic foraminiferal tests; one worm tube filled with calcite.	distal/ outer shelf	60	
Tuff	Tuff consists of altered volcanic glass with an intersertal texture; detritus grains (R): biotite (10 μm), ksp. (10 μm) and angular quartz (13 μm); Fossils (R): foraminifera tests; sponge spicules and broken shells.	basin	40	
Marlstone	Marlstone with a micrite–microsparite matrix; detritus grains (R), moderately to well sorted: feldspars (pl. (16–36 μm); ksp. (8–21 μm)); some are altered by sericite; lithic fragments of pl. (59–100 μm); angular to subrounded quartz (5–25 μm), some presents inclusions; biotite. Foraminiferal tests (F): globigerinid, gastropods and broken shells fragments. The organic matter is rare, and framboidal pyrite replaces some.		45, 50, 56	
	Marlstone with a microsparite and micrite matrix; detritus grains (R), poorly sorted: angular to rounded quartz (10–350 μm), ksp. (8–26 μm) few have inclusions, and some are altered by sericite; pl. (8 μm); lithic fragment of pl. (16 μm); biotite. Fossils (C): globigerinid, one test is destroyed and recrystallized; broken ostracods valves. The organic matter is rare, and some are replaced by pyrite or framboidal pyrite.	distal	30, 35, 25	
	Marlstone with a microsparite and micrite matrix; detritus grains (R): subrounded quartz (10–50 μm), pl. (14-25 μm); sericitized ksp. (300 μm); lithic fragments composed of quartz and feldspar (33–160 μm); some of the quartz has inclusions; Fossils (R): planktonic foraminifera, ostracods, gastropods, broken shells. The organic matter is frequent (sample 5) and can be observed a descending trend with height (sample 20).	basin	20, 15, 10, 5	
Sandy to silty marlstone	Silty marlstone with a microsparite matrix; detritus grains (C), well sorted: quartz subrounded (7–10 μm); ksp. (10 μm); calcite (12 μm). Foraminiferal tests (F), some have cherts or pyrite infills; globigerinid and ostracods valves; broken shells. The organic matter is scattered, some are replaced with framboidal pyrite.		1	
	Fossiliferous sandy marlstone with a micrite matrix; detritus grains (F), poorly sorted: feldspars ksp. (10–42 μm), some of them are altered by sericite; lithic fragments of ksp. (25–67 μm); and pl. (50 μm); quartz, chlorite/biotite. Fossils (A): globigerinid, one uniaxial foraminifera; one foraminifera filled with glauconite, two filled with chert; bryozoa; spicule; ostracods valves and shell fragments. The organic matter is scattered, and it is pyritized.		78, 75	Footwall Section

(A) - abundant, (F) - frequent, (C) - common, (R) - rare, ksp. - K-feldspar, pl. - Plagioclase, Env. - environment, No. - sample number.

The fine-grained upper part of the Footwall Section contains very low organic matter (avg. TOC: 0.27 %) and a type III–IV kerogen (HI: 23–104 mg HC/g TOC).

Microscopic observations show that the organic matter is dominated by vitrinite (~90 vol.%), whereas inertinite and liptinite are present in small amounts. Vitrinite reflectance of samples from the lower part of the Hanging Wall Section is about 0.3% R_r (sample 1: 0.31% R_r; sample 4: 0.30% R_r; sample 12: 0.29% R_r).

4.3. The molecular composition of hydrocarbons

Biomarker data were determined for seven samples from the organic matter-rich lower part of the Hanging Wall

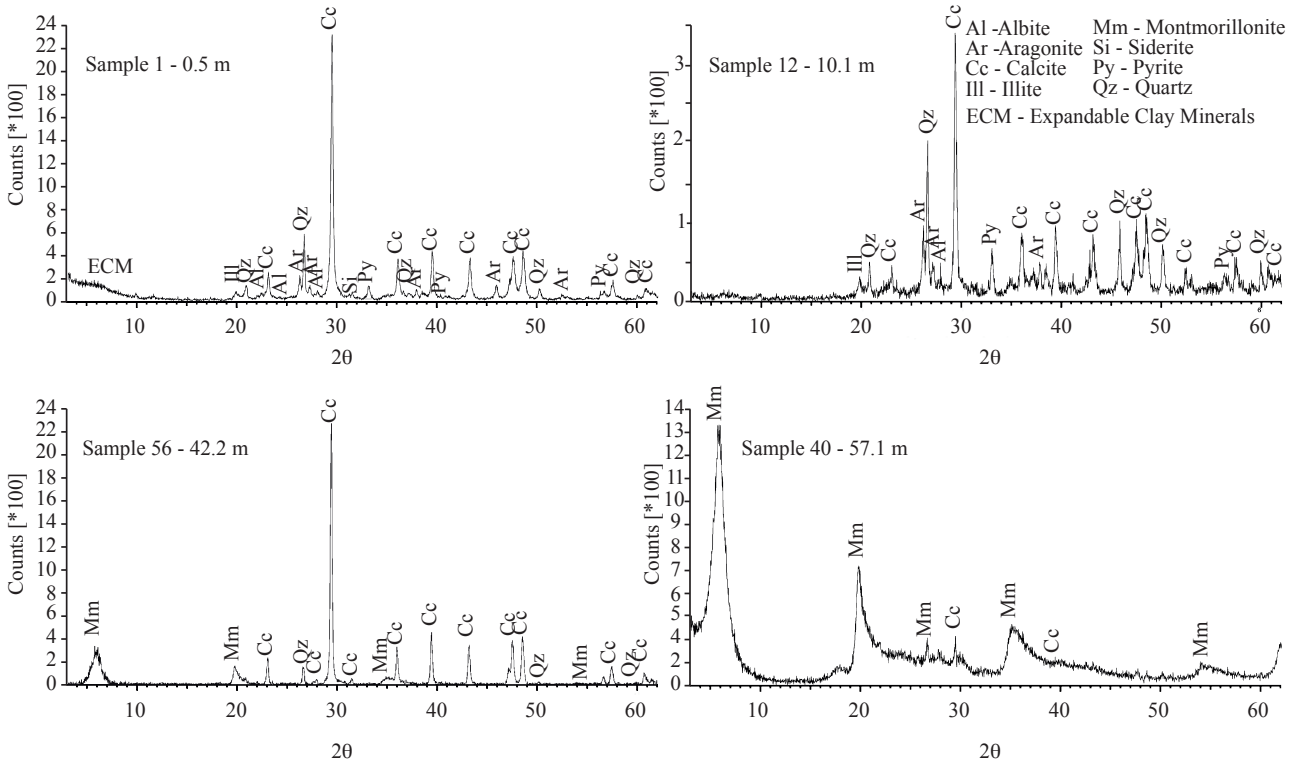

Figure 6. X-ray powder diffractograms of selected samples from the İhsaniye Formation (Hanging Wall Section): samples 1, 12, 56, and 40; (for samples position see Figure 4). Sample 40 represents the tuffaceous rock.

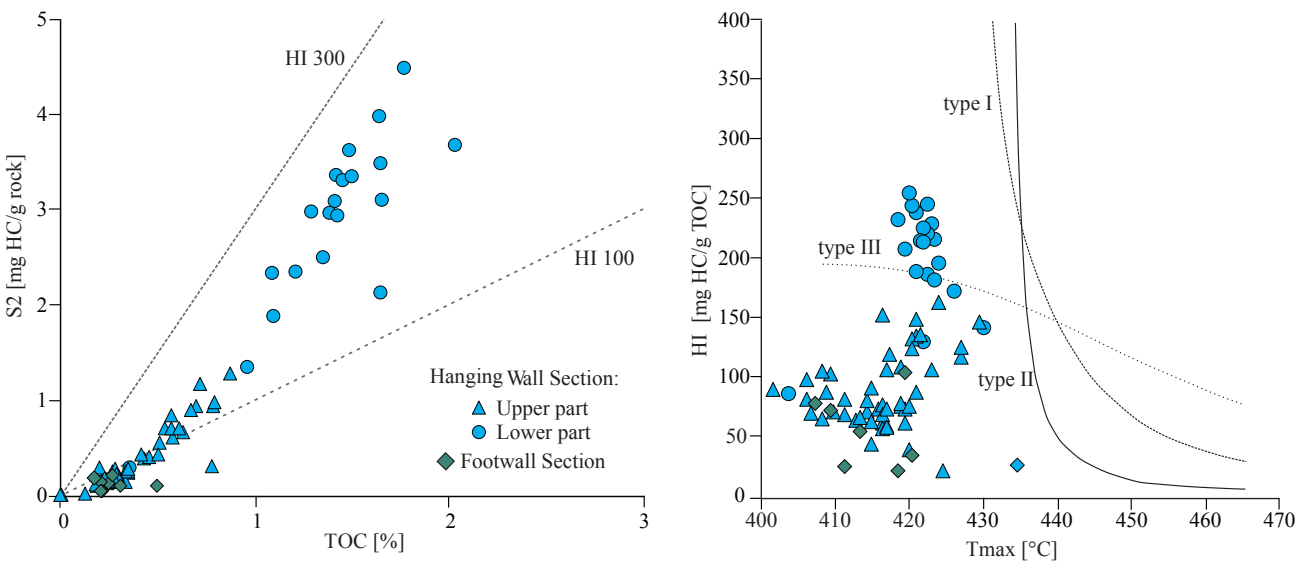

Figure 7. Plots of S2 vs. TOC and hydrogen index (HI) vs. Tmax for the İhsaniye Formation. The İhsaniye Formation contains type III and II kerogen.

Section and four samples with moderately high TOC contents (0.6–0.9 wt.%) from its upper part. Typical ion traces are listed in Table 2. The extractable organic matter (EOM) yields of the İhsaniye Formation vary between 1.12 and 2.82 mg/g TOC and are dominated by polar compounds (NSO, 62%–83% of EOM). In contrast, hydrocarbons are rare. Consequently, only selected biomarker ratios could be determined.

Table 2. Organic geochemical data of the İhsaniye Formation.

Sample no.	Height	TOC	HI	EOM	HC	NSO	Asph.	n-C_{15-20}	n-C_{21-25}	n-C_{26-32}	Pr/Ph	Ts/Tm	Steroids/ hopanoids	22S/ (22S+22R) C_{31}-Hopanes	Di/ (Di+Tri) terpeno.	Di+Tri-terpeno.	MPI index
	[m]	[wt%]	[mg/ gTOC]	[mg/ gTOC]	[%]											[µg/ gTOC]	
37	36.9	0.79	119	1.54	7	73	19	15	29	56	0.33	3.55	0.41	0.16	0.67	1.00	0.19
31	31.0	0.63	106	1.28	2	81	17	14	35	52	0.43	5.14	0.54	0.20	0.77	0.49	0.10
26	26.5	0.68	135	1.32	5	81	14	11	31	59	0.58	1.78	0.33	0	0.93	0.05	[0.49]
22	22.2	0.88	146	1.12	8	83	10	19	36	45	0.40	15.41	0.01	0	0.72	1.10	0.24
17	15.3	1.43	235	1.45	24	62	14	18	32	50	0.69	1.58	0.27	[0.42]	0.88	4.12	0.06
13	11.1	1.64	242	2.82	3	73	14	7	31	63	0.43	9.52	0.27	0.35	0.52	32.12	0.28
9	7.9	1.65	129	2.31	13	74	13	8	30	62	0.23	12.42	0.64	0.24	0.06	0.76	0.24
7	5.8	1.36	184	2.16	5	79	16	11	34	55	0.49	8.07	1.18	0.26	0.75	15.19	0.20
5	4.1	1.66	187	2.33	7	81	11	14	37	49	0.45	5.90	0.62	0.35	0.73	24.93	0.28
3	2.6	2.04	180	2.60	7	81	12	11	42	48	0.58	5.71	0.83	0.29	0.88	26.03	0.22
1	0.5	1.10	170	1.60	13	73	14	33	36	31	0.42	4.51	0.10	0.30	0.85	9.64	0.17

TOC - total organic carbon, HI - hydrogen index, EOM - extracted organic matter, HC - hydrocarbons yields, NSO - polar compounds, Asph. - asphalthene, n-C_{15-20} - short-chain alkanes, n-C_{21-25} - medium-chain alkanes, n-C_{26-32}- long-chain alkanes; Pr/Ph - Pristane/Phytane ratio; Di/(Di+Tri) terpeno. - Diterpenoids/triterpenoids ratio.

4.3.1. n-Alkanes and isoprenoids

The extracts from the İhsaniye Formation are dominated by long-chain n-alkanes (n-$C_{26–32}$: avg. 51.8%), which are characteristic for higher land plants (mainly plant waxes; Eglinton and Hamilton, 1967), and middle chain n-alkanes (n-$C_{21–25}$: avg. 33.9%), which may originate from aquatic macrophytes (Ficken et al., 2000). In contrast, short chain n-alkanes, typically related to algae and microorganisms, are rare (n-$C_{15–20}$: avg. 14.6%). There is a strong odd–even predominance with an average carbon preference index (Bray and Evans, 1961) of 6.9, typical for terrestrial land plants with low maturity.

Concentrations of pristane (Pr) and phytane (Ph) are very low, probably due to low maturity. Hence calculated Pr/Ph ratios (0.23–0.58) indicating anoxic conditions (Didyk et al., 1978) have to be treated with caution.

4.3.2. Steroids

The concentration of steroids is generally low (<2 μg/g TOC). C_{27} and C_{29} are visible in low amounts, while C_{28} steranes are missing. Sterenes, the immature precursor of steranes, are dominated by C_{29} sterenes with concentrations up to 0.4 μg/g TOC. Similar to the steranes, the C_{28} sterenes are nearly absent.

Steroids/hopanoids ratios range between 0.01 and 1.18. Values above 1 indicate organic matter input with a major contribution of marine algae, while values below 1 point to a dominantly land plant contribution (Moldowan and Wolfgang, 1985). Within the İhsaniye Formation, elevated values (1.18) are found only in one sample (7, 5.8 m) in the lower part of the section, whereas the entire section is dominated by a land plant contribution (0.01–0.83).

4.3.3. Terpenoids

Hopanes are nonaromatic cyclic triterpenoids that originate from precursors in bacterial membranes (Ourisson et al., 1979). Their concentration in the İhsaniye Formation is low (<2.6 μg/g TOC). The C_{31} 22S/(22S + 22R) hopane isomerization ratio varies widely between 0.0 and 0.42. Despite this variation, which may result from difficulties with quantification, the ratios indicate that the organic matter is immature (Peters et al., 2005). The ratio of C_{27} 18α-trisnorhopane (Ts) and C_{27} 17α-trisnorhopane (Tm) is a parameter dependent on both source and maturity (Moldowan and Fago, 1986). In the studied sample set, the Ts/Tm ratio ranges from 1.58 to 15.41. ββ-hopanes are highly specific for immature to early oil generation source rocks (Seifert and Moldowan, 1980) and occur in concentrations up to 1.4 μg/g TOC.

4.3.4. (Methyl-)Phenanthrenes

The phenanthrene concentration is <0.5 μg/g TOC. Except for two samples, the methylphenanthrene index (MPI-1) (Radke et al., 1980) is low (<0.28), reflecting the low maturity of the section. Higher values (~0.65) are found in samples with very low concentrations of phenanthrene and methylphenathrenes.

4.3.5. Land-plant related biomarkers

Bi- and tricyclic diterpenes can be used to determine terrestrial organic matter input (Simoneit et al., 1986). Phyllocladane and retene are gymnosperm-derived biomarkers and occur in concentrations up to 20.8 μg/g TOC, retene being the most abundant. Angiosperm-derived biomarkers (triterpenoids) like perylene, and olea-12-ene (<1.23 μg/g TOC) are far less abundant. A representative for land plant input is indicated by the sum of di- and triterpenoids and the di-/(di- + triterpenoids) ratio is representative for the ratio of gymnosperms to angiosperms (e.g., Bechtel et al., 2008). The sum of di- and triterpenoids is higher in the lower part of the section (max. 32.1 μg/g TOC) and lower in its upper part (max. 1.1 μg/g TOC). Except for sample 9, the di-/(di- + triterpenoids) ratio is high (0.52–0.93), indicating a significant contribution of gymnosperms to the terrestrial biomass.

4.4. Strontium isotope data

Strontium isotope (Sr^{86}/Sr^{87}) ratios were determined on foraminifera from 34 samples and range from 0.707742 to 0.708071 (Table 3). All but sample 33 fall within a much smaller range of 0.707742 to 0.707926. Sr isotope data are commonly used to generate an age for open-marine sediments (McArthur et al., 2012). However, because there is evidence to suggest that at times the basin was not connected to the global ocean, in this paper we use Sr isotope ratios combined with independent ages derived from the nannofossil assemblages to identify whether or not the basin was isolated from the open ocean. Within this context, Sr isotope ratios that plot within the error of coeval ocean water indicate that the basin was connected to the global ocean (Flecker and Ellam, 2006). The Sr isotope ratios are therefore plotted against the estimated age of each sample (Figure 8) as determined by assuming constant sedimentation rates between the biostratigraphic tie points identified by Simmons et al. (this volume). The more limited constraints on the exact stratigraphic position of the footwall samples mean that there is greater uncertainty in their age and hence the value of coeval ocean water Sr isotope ratio for these samples compared to those from the Hanging Wall Section.

Comparison with the global ocean Sr isotope record for this period (McArthur et al., 2012) illustrates that only five of the 34 samples give Sr isotope ratios within the error of ocean water values (Figure 8). All but one of the remaining samples have ratios lower than that for coeval ocean water (Figure 8), suggesting that the connection with the open ocean was substantially restricted or closed during deposition of most of the İhsaniye Formation.

Table 3. Strontium isotopes results.

NP	Height (m)	Sample	Approximate age	$^{87}Sr/^{86}Sr$	2σ
	Hanging Wall Section				
NP23	67.5	70	31.16	0.707909	0.000020
	66.2	68	31.20	0.707907	0.000023
	64.3	65	31.25	0.707872	0.000020
	61.6	62	31.33	0.707926	0.000020
	57.1	40	31.46	0.707887	0.000020
	55.0	43	31.53	0.707900	0.000020
	53.5	45	31.57	0.707870	0.000020
	51.7	47	31.62	0.707853	0.000020
	49.5	49	31.69	0.707857	0.000018
	47.8	51	31.74	0.707892	0.000020
	45.8	53	31.79	0.707920	0.000018
	44.8	54	31.82	0.707893	0.000020
	40.8	57	31.94	0.707877	0.000020
	40.0	58	31.96	0.707875	0.000020
NP22	38.1	38	32.02	0.707870	0.000020
	36.1	36	32.14	0.707831	0.000021
	33.3	33	32.31	0.708071	0.000020
	30.1	30	32.50	0.707831	0.000020
	27.2	27	32.67	0.707860	0.000020
	24.9	25	32.80	0.707845	0.000016
	23.0	23	32.92	0.707811	0.000020
NP21	21.9	21	32.96	0.707774	0.000020
	19.1	20	33.08	0.707817	0.000021
	16.2	18	33.21	0.707811	0.000020
	10.1	12	33.47	0.707742	0.000020
	8.3	10	33.54	0.707810	0.000017
	6.8	8	33.61	0.707831	0.000020
	4.1	5	33.72	0.707799	0.000020
	2.6	3	33.79	0.707822	0.000020
	0.5	1	33.88	0.707796	0.000018
	Footwall Section				
NP23	5.9	77		0.707886	0.000020
	4.8	75		0.707889	0.000020
	3.3	73		0.707908	0.000020
	1.7	71		0.707884	0.000020

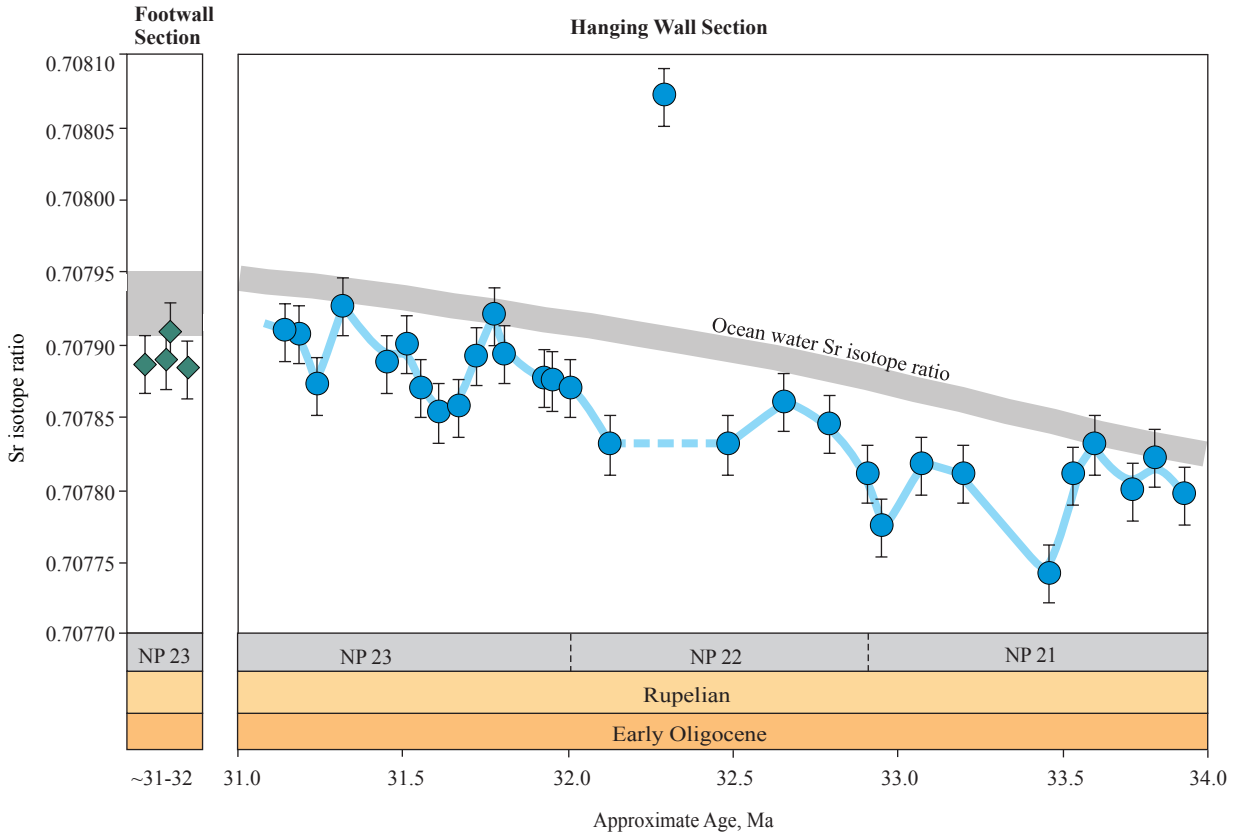

Figure 8. Variation in $^{87}Sr/^{86}Sr$ in the İhsaniye Formation along the Hanging Wall and Footwall sections. Ages for the samples are calculated assuming constant sedimentation rages between biostratigraphic boundaries as determined by Simmons et al. (this volume). The ocean water Sr isotope data are derived from McArthur et al. (2012). The thickness of the ocean water curve includes the analytical uncertainty.

5. Discussion

5.1. Maturity

The low Tmax values (~418 °C) in combination with vitrinite reflectance measurements (0.29%–0.31% R_r) show that the organic matter in the İhsaniye Formation is immature. This interpretation is supported by the occurrence of C_{29-31} ββ-hopanes, low hopane isomerization ratios (0.0–0.4), and low MPI-1 values (0.06–0.28).

5.2. Depositional environment

Apart from the results of the present study, the assessment of the depositional environment considers paleontological data from the Hanging Wall Section published by Simmons et al. (this volume) in a companion paper.

The presence of foraminifera in the entire section indicates a fully marine environment, which is also supported by the detected TOC/S values of the İhsaniye Formation. The further discussion is focused on the lower and upper parts of the Hanging Wall Section.

5.2.1. The lower part (0–19.5 m)

According to Simmons et al. (this volume), the lower part of the section was deposited during NP21 in a shallowing bathyal to outer neritic environment. High percentages of quartz and land plant-derived macerals indicate strong detrital input. Simmons et al. (this volume) describe *Hoeglundina elegans*, an aragonite foraminifera species that can tolerate low oxygen water with low nutrient conditions. We speculate that the high amount of aragonite in this part of the section reflects the presence of *H. elegans*. Low oxygen conditions are also supported by relatively high TOC contents. Petrographic and organic geochemical data prove that organic matter is dominated by higher land plants. Strong terrestrial input is also supported by the abundant presence of pollen derived from gymnosperms and angiosperms (Simmons et al., this volume). Hence, the relatively low amount of aquatic organisms may be caused by oligotrophic conditions.

5.2.2. The upper part (19.5–68 m)

Simmons et al. (this volume) dated the upper part into the uppermost NP21 to lower NP23. Based on the ratio of planktonic and benthic foraminifera, these authors determined a deepening trend between samples 20 (19.1 m) and 55 (43.7 m). This trend is reflected by an upward

decrease in quartz/clay minerals ratios (Figure 4) and an upward decrease in the size of lithic fragments (from 300 µm to 60 µm). The presence of micrite is an indication of a low-energy depositional environment (Flügel, 2004). An increasing distance to the shoreline is also indicated by the decrease in organic matter, dominated by land plants.

Above sample 55 (44.7 m) quartz/clay minerals ratios (Figure 4) and the percentage of planktonic foraminifera remain stable (Simmons et al., this volume). Only the uppermost two samples have high quartz/clay minerals ratios, indicating stronger detrital input. Simmons et al. (this volume) suggest that this part of the section was deposited during a highstand systems tract. Organic matter contents remain very low (~0.3%), indicating a distal position to the shoreline as well as low productivity of aquatic organic matter and poor preservation conditions. Deposition of the tuffaceous rocks did not affect TOC contents, indicating that the increased nutrient availability did not cause algal blooms.

5.3. Comparison to coeval sediments in the Western Black Sea and the Thrace Basin

Typically, the Lower Oligocene succession in the Paratethys starts with marly sediments, which are overlain by thin carbonate-free shales or cherts (e.g., Sachsenhofer et al., 2018a, 2018b). Above this succession, a carbonate-rich layer forms a widespread marker horizon and represents the maximum of the isolation of the Paratethys ("Solenovian Event") during the early NP23 (e.g., Voronina and Popov, 1984; Rusu, 1999). Above follow largely carbonate-free shales. Marls representing the low salinity "Solenovian Event" have also been detected in the Western Black Sea (Sachsenhofer et al., 2009, 2018a, 2018b), including the well Ropotamo-1 (Mayer et al., 2018; for the position of the Ropotamo well see Figure 1).

Based on the age of the sediments, the Solenovian event is expected in the upper part of the Karaburun section dated as NP23 (40.0–67.5 m; samples 58–70; Figure 4). However, foraminiferal data (Simmons et al., this volume) and geochemical evidence (TOC/S ratio) exclude the presence of a major change in salinity. It cannot be completely excluded though that the Solenovian event follows above the exposed succession in the Karaburun area.

Sr isotope data suggest that the connection was at best transient only, and for most of the time there can only have been a restricted connection. Hence, a closer look at the Oligocene successions in the Çatalca gap and the Thrace Basin is necessary. Within this context, it is intriguing that the Pınarhisar Formation deposited at the margin of the Çatalca gap (Figure 1) contains endemic Solenovian mollusk fauna (Popov et al., 1985; Nevesskaja et al., 1987). Based on this mollusk fauna, Popov et al. (1985) and Nevesskaja et al. (1987) postulated brackish conditions. In contrast, based on the occurrence of Solenovian oolite shoals, İslamoğlu et al. (2010) assumed a marine and partially hypersaline environment with carbonate oversaturated waters. Nevertheless, all previous authors agree that the Pınarhisar Formation formed within the isolated Paratethys. However, as the Pınarhisar Formation accumulated at the shallow margin of the Çatalca gap, it is likely that it was restricted.

Gürgey and Batı (2018) studied the Lower Oligocene succession, up to 2500-m thick, in the center of the Thrace Basin. They distinguished a Pshekhian(?) Lower Mezardere Formation (NP21–22) deposited in neritic normal marine environments and a Solenovian Upper Mezardere Formation (NP23/24), which represents a slightly shallower neritic environment. Based on the presence of marine dinocysts (e.g., *Wetzeliella gochtii*) and high amounts of green algae (e.g., *Pediastrum* spp.), Gürgey and Batı (2018) argued for a brackish-marine environment. Hence, it is not clear if a marine connection through the Thrace Basin existed in Solenovian time and more information on the Solenovian succession in the Thrace Basin is needed.

The Sr isotope data from our samples suggest that no permanent connection between this area and the open ocean existed. Rather, for much of the time during deposition of the İhsaniye Formation, the connection with the global ocean was highly restricted with only transient episodes of sufficient open-ocean water to cause the Sr isotope ratio of Thrace Basin water to mirror that of coeval ocean water (Figure 8). The predominance of Sr isotope ratios lower than coeval ocean water suggests that fluvial or groundwater inputs had lower Sr isotope ratios. This is in line with more recent records from this area of the Black Sea, where the fluvial Sr isotope data are substantially lower than these ocean water values (e.g., Major et al., 2002, 2006). However, evidence of limited and episodic ocean water input does not necessarily equate to low salinity conditions since evaporation is driven by both freshwater dilution of ocean water and evaporation so that where the net evaporative flux is positive normal marine or even higher salinities can prevail despite a preponderance of freshwater input (Flecker et al., 2002; Topper et al., 2011).

5.4. Source rock potential

Potential source rocks in the İhsaniye Formation are restricted to its lower part (NP21). They contain TOC contents up to 2% and a type III–II kerogen (Figure 7), which is mainly gas prone and may generate minor liquid hydrocarbons only. Based on TOC contents, the source rocks may be classified as good (Figure 9). However, based on petroleum potential (S1 + S2), they are classified only as poor to fair source rocks.

This is also reflected in the source potential index, which was calculated according to Demaison and Huizinga

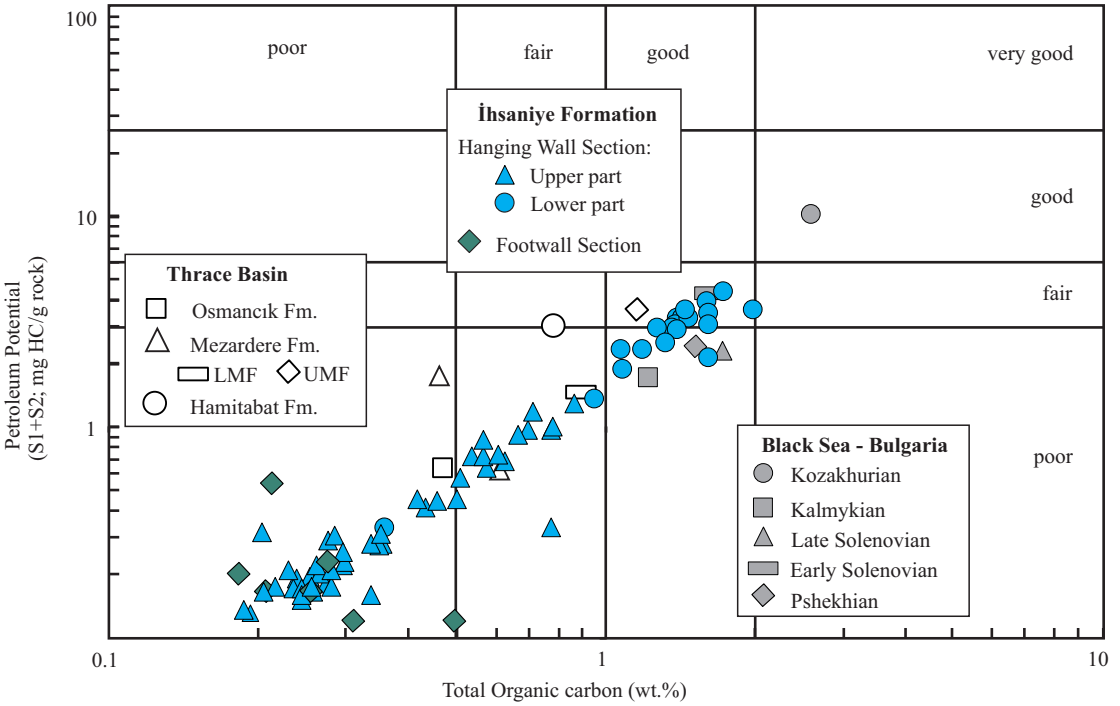

Figure 9. Petroleum potential of the İhsaniye Formation. Mean values of the petroleum potential of sediments in the Thrace Basin and the Bulgarian part of the Black Sea are shown for comparison (data compiled from Sarı and Savan, 2008; Gürgey, 2009; Gurgey and Batı, 2018; Mayer et al., 2018). LMF - Lower Mezardere Formation, UMF - Upper Mezardere Formation.

(1994) (SPI = thickness × (S1 + S2) × bulk density/1000). For the calculation, only the lower organic matter-rich part (samples 1–19), 17.5-m thick, is considered. The net mudstone thickness and the density are estimated as 15 m and 2.55 g/cm^3, respectively. Considering an average S1 of 0.07 mg HC/g rock and an average S2 of 2.99 mg HC/g rock, the SPI is calculated as 0.14 t HC/m^2, which is a very low value. Hence, the source rock potential of the İhsaniye Formation is considered poor.

5.5. Comparison of the petroleum potential of Lower Oligocene rocks in the Western Black Sea and the Thrace Basin

Mayer et al. (2018) studied the petroleum potential of Pshekhian and Solenovian (Early Oligocene) rocks in the Western Black Sea Basin, offshore Bulgaria. They showed that the average TOC contents of Pshekhian and Solenovian rocks are in the order 1.5 to 1.7 wt.%, but that HI values are higher in the Lower Solenovian (270 mg HC/g TOC) than in underlying (160 mg HC/g TOC) and overlying units (130 mg HC/g TOC). Consequently, the petroleum potential of Lower Solenovian rocks is better than that of Pshekhian and Upper Solenovian units (Figure 9). This is also the case for the Ropotamo well, located relatively near the Karaburun area (Mayer et al., 2018).

Gürgey and Batı (2018) observed a similar trend in deep wells in the central Thrace Basin. Here the Pshekhian Lower Mezardere Formation contains a lower hydrocarbon potential (avg. TOC: 0.88 wt.%; max. 1.50 wt.%; avg. HI: 136 mg HC/g TOC; max 345 mg HC/g TOC) than the Solenovian Upper Mezardere Formation (avg. TOC: 1.15 wt.%; max. 1.86 wt.%; avg. HI: 285 mg HC/g TOC; Figure 9). Remarkable are partly very high HI values (up to 744 mg HC/g TOC) in the Upper Mezardere Formation, which have not been observed in any other Oligocene succession in the Black Sea area (Sachsenhofer et al., 2018a, 2018b).

For the sake of completeness, it should be added that the best source rocks units in the Western Black Sea Basin are Lower Miocene diatom-rich rocks, which accumulated within shelf-break canyons (avg. 2.6 wt.% TOC, avg. HI: 400 mg HC/g TOC; Mayer et al., 2018; Figure 9). In contrast, the best source rocks in the Thrace Basin are found in the Middle to Upper Eocene Hamitabat Formation (avg. 0.78 wt.% TOC; max. 9.96 wt.%). Average S1 + S2 is 3.29 mg HC/rock (Figure 9), and the presence of type III kerogen classifies the Hamitabat Formation as gas-prone (Gürgey, 2009). The Oligocene Osmancık Formation (avg. 0.47 wt.% TOC, max. wt.% 1.75 wt.% TOC, S1 + S2 0.62 mg HC/rock) can locally reach fair hydrocarbon potential (Sarı and Savan, 2008; Şen, 2011; Figure 9).

Although the İhsaniye Formation is located between the two basins, the majority of the samples analyzed have a poor hydrocarbon potential (Figure 9). Only samples from

the lower part of the Pshekhian succession (NP21; 0–19.5 m) have a fair potential, similar to that observed in coeval strata in the West Black Sea Basin and the Thrace Basin.

6. Conclusions

The İhsaniye Formation is exposed along the Black Sea shore in 50-m-high cliffs and includes fine-grained sediments overlain by thick mass transport sediments. The study focused on fine-grained sediments deposited on the hanging wall side of a syn-sedimentary normal fault ("Hanging Wall Section"), where the İhsaniye Formation is about 70-m thick. The results allow the following conclusions:

The fine-grained part of the İhsaniye Formation is represented by an alternation of marl, carbonate-rich siltstone, sandstone, and tuffaceous beds and the frequency of the sandy layers intercalations is decreasing higher in the stratigraphy.

The TOC/S values of the İhsaniye Formation together with the continuous presence of the foraminifera in the studied section indicate a fully marine environment. The Hanging Wall Section is divided into two parts: the lower part (0–19.5 m) contains relatively high amounts of terrestrial organic matter deposited in oxygen-depleted conditions, while the upper part (19.5–68 m) contains a prominent tuff layer. The succession below the tuff layer is low in organic matter (avg. TOC: 0.38%) and reveals a deepening trend in a low-energy depositional environment. The deepening trend is reflected by an upward decrease in detrital organic and inorganic matter.

In comparison with the coeval sediments in the Western Black Sea and the Thrace Basin, the İhsaniye Formation shows a different evolution, in which the low salinity "Solenovian Event" is missing even though the Sr isotope record suggests that full connection with the Mediterranean occurred for relatively short periods during this interval. One possible explanation is that the "Solenovian Event" is hidden within the overlying mass transport sediments.

The studied succession is immature. The TOC content reaches a maximum of 2.04 wt.% in the lower part of the succession (0–19.5 m), which has some hydrocarbon potential even though it is poor. If mature, the section may generate 0.14 t HC/m^2. The presence of type III–II kerogen indicates that the rocks are gas prone and may generate minor liquid hydrocarbons only.

Acknowledgments

This work is part of the PhD thesis by Emilia Tulan at Montanuniversitaet Leoben (Chair of Petroleum Geology) in Austria, and it is supported by the OMV Group - Technology project. Help during field work by Aral Okay, Jan Mayer, and Mike Simmons is highly appreciated. Mike Simmons also is thanked for providing invaluable paleontological insights and for useful discussions. Anne Kelly, Vincent Gallagher, and Kathy Keefe are thanked for conducting the Sr isotope analyses at SUERC. We are indebted to Ercan Özcan and Mike Simmons for their constructive feedback, which helped greatly to improve the manuscript.

References

Akartuna M (1953). Geology of Çatalca-Karacaköy Region. University of İstanbul, İstanbul Üniversitesi Fen Fakülesi Monografileri 13: 88 (in Turkish).

Bailey TR, McArthur JM, Prince H, Thirlwall MF (2000). Dissolution methods for strontium isotope stratigraphy: whole rock analysis. Chemical Geology 167 (3-4): 313-319. doi: 10.1016/s0009-2541(99)00235-1

Barker S, Greaves M, Elderfield H (2003). A study of cleaning procedures used for foraminiferal Mg/Ca paleothermometry. Geochemistry, Geophysics, Geosystems 4 (9): 1-20. doi: 10.1029/2003gc000559

Bechtel A, Gratzer R, Sachsenhofer RF, Gusterhuber J, Lücke A et al. (2008). Biomarker and carbon isotope variation in coal and fossil wood of Central Europe through the Cenozoic. Palaeogeography, Palaeoclimatology, Palaeoecology 262 (3-4): 166-175. doi: 10.1016/j.palaeo.2008.03.005

Bray EE, Evans ED (1961). Distribution of n-paraffins as a clue to recognition of source beds. Geochimica et Cosmochimica Acta 22 (1): 2-15. doi: 10.1016/0016-7037(61)90069-2

Burkan K (1992). Geochemical evaluation of the Thrace Basin. Proceedings of the 9th Petroleum Congress of Turkey 48: 34.

Chatalov GA (1988). Recent developments in the geology of the Strandzha Zone in Bulgaria. Bulletin of the Technical University of İstanbul 41: 433-465.

Cheshitev G, Kancev I (1989). Geological map of People`s Republic of Bulgaria. 1:500.000. Committee of Geology, Department of Geophysical Prospecting and Geological Mapping, Sofia, Bulgaria.

Demaison G, Huizinga BJ (1994). Genetic classification of petroleum systems using three factors: charge, migration and entrapment. AAPG Memoirs 60: 73-92.

Didyk BM, Simoneit BR, Brassell ST, Eglinton G (1978). Organic geochemical indicators of paleoenvironmental conditions of sedimentation. Nature 272 (5650): 216-222. doi: 10.1038/272216a0

Eglinton G, Hamilton RJ (1967). Leaf epicuticular waxes. Science 156 (3780): 1322-1335. doi: 10.1126/science.156.3780.1322

Ficken KJ, Li B, Swain DL, Eglinton G (2000). An n-alkane proxy for the sedimentary input of submerged/floating freshwater aquatic macrophytes. Organic Geochemistry 31 (7-8): 745-749. doi: 10.1016/s0146-6380(00)00081-4

Flecker R, De Villiers S, Ellam RM (2002). Modelling the effect of evaporation on the salinity - $^{87}Sr/^{86}Sr$ relationship in modern and ancient marginal-marine systems: the Mediterranean Messinian Salinity Crisis. Earth and Planetary Science Letters 203 (1): 221-233. doi: 10.1016/s0012-821x(02)00848-8

Flecker R, Ellam RM (2006). Identifying Late Miocene episodes of connection and isolation in the Mediterranean-Paratethyan realm using Sr isotopes. Sedimentary Geology 188-189: 189-203. doi: 10.1016/j.sedgeo.2006.03.005

Flügel E (2004). Microfacies of Carbonate Rocks: Analysis, Interpretation and Application. Berlin, Germany: Springer Science and Business Media. doi: 10.5860/choice.42-3437

Gedik İ, Timur E, Umut M, Bilgin AZ, Pehlivan Ş et al. (2014). Geological Maps of Turkey, 1:50.000 scale İstanbul F21-a sheet and explanatory notes. Ankara, Turkey: Maden Tetkik ve Arama Genel Müdürlüğü.

Gürgey K (1999). Geochemical characteristic and thermal maturity of oils from the Thrace basin (western Turkey) and western Turkmenistan. Journal of Petroleum Geology 22 (2): 167-189. doi: 10.1111/j.1747-5457.1999.tb00466.x

Gürgey K (2009). Geochemical overview and undiscovered gas resources generated from Hamitabat petroleum system in the Thrace Basin, Turkey. Marine and Petroleum Geology 26 (7): 1240-1254. doi: 10.1016/j.marpetgeo.2008.08.007

Gürgey K, Batı Z (2018). Palynological and petroleum geochemical assessment of the Lower Oligocene Mezardere Formation, Thrace Basin, NW Turkey. Turkish Journal Earth Sciences 27 (5): 349-383. doi: 10.3906/yer-1710-24

Gürgey K, Philp RP, Emiroglu H, Siyako M, Uygur E et al. (2003). Geochemical characterization of natural gas; n-alkane carbon isotope approach and its implication to source, maturity, migration, and mixing deductions. Proceedings of the 14th International Petroleum Congress and Exhibition of Turkey, pp. 174.

Gürgey K, Philp RP, Emiroglu H, Siyako M, Uygur E et al. (2005). Geochemical and isotopic approach to maturity/source/mixing estimations for natural gas and associated condensates in the Thrace basin, Turkey. Applied Geochemistry 20 (11): 2017-2037. doi: 10.1016/j.apgeochem.2005.07.012

Hans U, Kleine T, Bourdon B (2013). Rb-Sr chronology of volatile depletion in differentiated protoplanets: BABI, ADOR and ALL revisited. Earth and Planetary Science Letters 374: 204-214. doi: 10.1016/j.epsl.2013.05.029

Horwitz Philip E, Chiarizia R, Dietz ML (1992). A novel strontium-selective extraction chromatographic resin. Solvent Extraction and Ion Exchange 10 (2): 313-336. doi: 10.1080/07366299208918107

Horwitz Philip E, Dietz ML, Fisher DE (1991). Separation and preconcentration of strontium from biological, environmental, and nuclear waste samples by extraction chromatography using a crown ether. Analytical Chemistry 63 (5): 522-525. doi: 10.1021/ac00005a027

Hoşgörmez H, Yalçın MN, Cramer B, Gerling P, Mann U (2005). Molecular and isotopic composition of gas occurrences in the Thrace basin (Turkey): origin of the gases and characteristics of possible source rocks. Chemical Geology 214 (1-2): 179-191. doi: 10.1016/j.chemgeo.2004.09.004

Huvaz O, Karahanoglu N, Ediger V (2007). The thermal gradient history of the Thrace Basin, NW Turkey: correlation with basin evolution process. Journal of Petroleum Geology 30 (1): 3-24. doi:10.1111/j.1747-5457.2007.00003.x

İslamoğlu Y, Harzhauser M, Gross M, Jiménez-Moreno G, Ćorić S et al. (2010). From Tethys to Eastern Paratethys: Oligocene depositional environments, paleoecology and paleobiogeography of the Thrace Basin (NW Turkey). International Journal of Earth Science 99 (1): 183-200. doi: 10.1007/s00531-008-0378-0

Lafargue E, Marquis F, Pillot D (1998). Rock-Eval 6 applications in hydrocarbon exploration, production, and soil contamination studies. Revue de l'institut français du pétrole 53 (4): 421-437. doi: 10.2516/ogst:1998036

Less G, Özcan E, Okay AI (2011). Stratigraphy and larger foraminifera of the Middle Eocene to Lower Oligocene shallow-marine units in the northern and eastern parts of the Thrace Basin, NW Turkey. Turkish Journal of Earth Sciences 20 (6): 793-845. doi: 10.3906/yer-1010-53

Major CO, Goldstein SL, Ryan WBF, Lericolais G, Piotrowski AM et al (2006). The co-evolution of Black Sea level and composition through the last deglaciation and its paleoclimatic significance. Quaternary Science Reviews 25 (17-18): 2031-2047. doi: 10.1016/j.quascirev.2006.01.032

Major CO, Ryan WBF, Lericolais G, Hajdas I (2002). Constraints on Black Sea outflow to the Sea of Marmara during the last glacial-interglacial transition. Marine Geology 190 (1-2): 19-34. doi:10.1016/s0025-3227(02)00340-7

Mattinson JM (1972). Preparation of hydrofluoric, hydrochloric, and nitric acids at ultralow lead levels. Analytical Chemistry 44 (9): 1715-1716. doi: 10.1021/ac60317a032

Mayer J, Rupprecht BJ, Sachsenhofer RF, Tari G, Bechtel A et al. (2018). Source potential and depositional environment of Oligocene and Miocene rocks offshore Bulgaria. Geological Society, London, Special Publications 464 (1): 307-328. doi: 10.1144/sp464.2

McArthur JM, Howarth RJ, Shields GA (2012). Strontium isotope stratigraphy. In: Gradstein FM, Ogg JG, Schmitz M, Ogg G (editors). The Geologic Time Scale. Amsterdam, the Netherlands: Elsevier, pp. 127-144. doi: 10.1016/b978-0-444-59425-9.00007-x

Moldowan MJ, Wolfgang K (1985). Relationship between petroleum composition and depositional environment of petroleum source rocks. AAPG Bulletin 69 (8): 1255. doi: 10.1306/ad462bc8-16f7-11d7-8645000102c1865d

Moore LJ, Murphy TJ, Barnes IL, Paulsen PJ (1982). Absolute isotopic abundance ratios and atomic weight of a reference sample of strontium. Journal of Research of the National Bureau of Standards 87 (1): 1. doi: 10.6028/jres.087.001

Natal'in B, Say AG (2015). Eocene - Oligocene stratigraphy and structural history of the Karaburun area, southwestern Black Sea coast, Turkey: transition from extension to compression. Geological Magazine 152: 1104-1122. doi:10.1017/s0016756815000229

Nevesskaja LA, Goncharova IA, Iljina LB, Paramonova NP, Popov SV et al. (1987). History of the Paratethys. Ann Instituti Geologici Publici Hungarici 70: 337-342.

Nier AO (1938). The isotopic constitution of strontium, barium, bismuth, thallium and mercury. Physical Review 54 (4): 275-278. doi: 10.1103/physrev.54.275

Okay A, Özcan E, Hakyemez A, Siyako M, Sunal G et al. (2019). The Thrace Basin and the Black Sea: the Eocene-Oligocene marine connection. Geological Magazine 156 (23): 39-61. doi: 10.1017/S0016756817000772

Okay A, Şengör AM, Görür N (1994). Kinematic history of the opening of the Black Sea and its effect on the surrounding regions. Geology 22 (3): 267-270. doi: 10.1130/0091-7613(1994)022<0267:KHOTOO>2.3.CO;2

Okay AL, Satır M, Tüysüz O, Akyüz S, Chen F (2001). The tectonics of the Strandja Massif: late-Variscan and mid-Mesozoic deformation and metamorphism in the northern Aegean. International Journal of Earth Sciences 90 (2): 217-233

Oktay F, Eren RH, Sakınç M (1992). Sedimentary geology of eastern Thrace Oligocene Basin around Karaburun-Yeniköy. In Proceedings of the 9th Petroleum Congress of Turkey. Ankara, Turkey: Turkish Association of Petroleum Geologists 92-101 (in Turkish).

Ourisson G, Albrecht P, Rohmer M (1979). The Hopanoids: palaeochemistry and biochemistry of a group of natural products. Pure and Applied Chemistry 51 (4): 709-729. doi: 10.1351/pac197951040709

Peters KE, Walters CC, Moldowan JM (2005). The Biomarker Guide Volume 1: Biomarkers and Isotopes in the Environment and Human History. Cambridge. UK: Cambridge University Press. doi: 10.1017/s0016756806212056

Pin C, Briot D, Bassin C, Poitrasson F (1994). Concomitant separation of strontium and samarium-neodymium for isotopic analysis in silicate samples, based on specific extraction chromatography. Analytica Chimica Acta 298 (2): 209-217. doi: 10.1016/0003-2670(94)00274-6

Popov SV, Iliana LB, Nikolayeva YA (1985). Molluscs and ostracods from the Oligocene Solenovian horizon of the Eastern Paratethys. Paleontological Journal 1: 28-41 (in Russian).

Popov SV, Rögl F, Rozanov AY, Steininger FF, Shcherba IG et al. (2004). Lithological-Paleogeographic maps of Paratethys - 10 maps Late Eocene to Pliocene. Stuttgart, Germany: Schweizerbart'sche Verlagsbuchhandlung.

Popov SV, Voronina AA, Gontscharova IA (1993). Stratigraphy and bivalves of the Oligocene-Lower Miocene of the Eastern Paratethys. Moscow, Russia: Publications of the Paleontological Institute, 256, Russian Academy of Sciences, (in Russian).

Pupp M, Bechtel A, Ćorić S, Gratzer R, Rustamov J et al. (2018). Eocene and Oligo-Miocene Source Rocks in the Rioni and Kura basins of Georgia: depositional environment and petroleum potential. Journal of Petroleum Geology 41 (3): 367-392. doi: 10.1111/jpg.12708

Radke M, Willsch H, Welte DH (1980). Preparative hydrocarbon group type determination by automated medium pressure liquid chromatography. Analytical Chemistry 52 (3): 406-411. doi: 10.1021/ac50053a009

Rusu A (1999). Rupelian mollusk fauna of Solenovian type found in Eastern Carpathians (Romania). Acta Palaeontologica Romaniae 2: 449-452.

Sachsenhofer RF, Popov SV, Bechtel A, Ćorić S, Francu J et al. (2018a). Oligocene and Lower Miocene source rocks in the Paratethys: palaeogeographic and stratigraphic controls. In: Simmons M (editor). Petroleum Geology of the Black Sea. Geological Society Special Publication 464 (1): 267-306. doi: 10.1144/sp464.1

Sachsenhofer RF, Popov SV, Ćorić, S, Mayer J, Misch D et al. (2018b). Paratethyan petroleum source rocks: an overview. Journal of Petroleum Geology 41: 219-245. doi: 10.1111/jpg.12702

Sachsenhofer RF, Stummer B, Georgiev G, Dellmour R, Bechtel A et al. (2009). Depositional environment and hydrocarbon source potential of the Oligocene Ruslar Formation (Kamchia Depression; Western Black Sea). Marine and Petroleum Geology 26 (1): 57-84. doi: 10.1016/j.marpetgeo.2007.08.004

Sakınç M (1994). Karaburun (B İstanbul) denizel oligoseninin stratigrafisi ve paleontolojisi. Maden Tetkik ve Arama Dergisi 116: 9-14.

Sancay HR, Batı Z. Late Eocene to Early Oligocene palynostratigraphy of the Western Black Sea, Eastern Paratethys. Turkish Journal of Earth Sciences (this volume).

Sarı A, Savan AK (2008). Organic Geochemical Investigations of the Tertiary Units in the Thrace Basin (Edirne, Turkey). Petroleum Science and Technology 6 (3): 322-345. doi: 10.1080/10916460600809485

Schultz LG (1964). Quantitative interpretation of mineralogical composition from X-ray and chemical data for the Pierre Shale, United States. Geological Survey Professional Paper. doi: 10.3133/pp391c

Sedat I, Yalçın MN (1997). Evolution of the thermal maturity in the Thrace Basin: revisited. Turkish Journal of Earth Sciences 6: 21-31.

Seifert WK, Moldowan JM (1980). The effect of thermal stress on source-rock quality as measured by hopane stereochemistry. Physics and Chemistry of the Earth 12: 229-237. doi: 10.1016/0079-1946(79)90107-1

Şen Ş (2011). Petroleum Source Rock Assessment of the Southwestern Thrace Basin, NW Turkey. Energy Sources, Part A: Recovery, Utilization, and Environmental Effects 33 (11): 1005-1017. doi:10.1080/15567036.2010.485177

Simmons MD, Bidgood MD, Connel PG, Ćorić S, Okay AI et al. Biostratigraphy and paleoenvironments of the Oligocene succession (İhsaniye formation) at Karaburun (NW Turkey). Turkish Journal of Earth Sciences (this volume).

Simmons MD, Tari GC, Okay AI (2018). Petroleum geology of the Black Sea: introduction. Geological Society, London, Special Publication 464 (1): 1-18. doi: 10.1144/sp464.15

Simoneit BRT, Grimalt JO, Wang TG, Cox RE, Hatcher PG et al. (1986). Cyclic terpenoids of contemporary resinous plant detritus and of fossil woods, ambers and coals. Organic Geochemistry 10 (4-6): 877-889. doi: 10.1016/s0146-6380(86)80025-0

Steiger RH, Jäger E (1977). Subcommission on geochronology: convention on the use of decay constants in geo- and cosmochronology. Earth and Planetary Science Letters 36 (3): 359-362. doi: 10.1016/0012-821x(77)90060-7

Taylor GH, Teichmüller M, Davis A, Diessel CFK, Littke R et al. (1998). Organic Petrology. Berlin, Germany: Gebrüder Borntaeger.

Topper RPM, Flecker R, Meijer PT, Wortel MJR (2011). A box model of the Late Miocene Mediterranean Sea: implications from combined $^{87}Sr/^{86}Sr$ and salinity data. Paleoceanography 26 (3) PA. doi: 10.1029/2010pa002063

Voronina AA, Popov SV (1984). Solenovian horizon from Eastern Paratethys. Bulletin of the Academy of Sciences of the USSR. Ser Geology 9: 41-53 (in Russian).

Yücel AO, Özcan E, Erbil Ü. Latest Priabonian larger benthic foraminiferal assemblages at the demise of the Soğucak Carbonate Platform (Thrace Basin and Black Sea shelf, NW Turkey): implications for shallow marine biostratigraphy. Turkish Journal of Earth Sciences (this volume).

Yurtsever A, Çağlayan A (2002). Geological maps of Turkey, 1:100.000 scale, İstanbul F21 and G21 sheet and explanatory text. Ankara, Turkey: Maden Tetkik ve Arama Genel Müdürlüğü.

Appendix: Bulk parameters of the İhsaniye Formation.

NP	Sample no.	Height	S1	S2	Tmax	TOC	S	PI	HI	TOC/ S	Calc. Equiv.
		[m]	[mg HC/g rock]		[°C]	[%]	[%]	[-]	[mgHC/ g TOC]	[-]	[%]
	Hanging Wall Section										
NP23	70	67.5	0.01	0.17	416	0.27	0.19	0.06	62	1.40	53.0
	69	67.0	0.01	0.14	416	0.24	0.21	0.07	58	1.17	48.8
	68	66.2	0.03	0.26	414	0.36	0.22	0.09	72	1.63	34.7
	67	65.8	0.01	0.16	417	0.26	0.20	0.06	60	1.27	41.2
	66	65.1	0.01	0.18	419	0.24	0.20	0.05	76	1.18	58.7
	65	64.3	0.01	0.19	416	025	0.26	0.05	73	0.95	49.2
	64	63.1	0.01	0.17	416	0.22	0.30	0.06	77	0.71	57.5
	63	62.9	0.01	0.16	416	0.23	0.20	0.06	69	1.17	57.1
	62	61.6	0.01	0.12	415	0.19	0.26	0.08	63	0.73	59.0
	61	60.9	0.01	0.16	408	0.24	1.47	0.06	66	0.17	40.7
	60	59.9	0.02	0.19	407	0.27	0.58	0.08	70	0.46	35.2
	59	59.0	0.02	0.27	406	0.27	0.51	0.07	98	0.54	33.1
	39	58.0	0.02	0.03	452	0.01	0.00	0.38			0.9
	40	57.1	0.01	0.02	408	0.00	0.01	0.33		0.79	0.6
	41	56.8	0.01	0.03	424	0.13	0.17	0.25	23	0.78	0.0
	42	55.9	0.02	0.26	419	0.35	0.43	0.05	74	0.82	42.5
	43	55.0	0.01	0.15	415	0.34	0.23	0.06	44	1.47	51.5
	44	54.5	0.02	0.31	416	0.20	0.51	0.05	152	0.39	40.1
	45	53.5	0.01	0.17	413	0.26	0.33	0.06	65	0.77	40.5
	46	52.5	0.03	0.95	421	0.71	0.79	0.03	134	0.90	54.0
	47	51.7	0.02	0.27	419	0.34	0.34	0.05	79	1.00	38.4
	48	50.4	0.01	0.16	420	0.20	0.16	0.06	76	1.27	61.6
	49	49.5	0.01	0.15	419	0.24	0.21	0.06	62	1.16	53.1
	50	48.6	0.01	0.21	414	0.26	0.41	0.05	81	0.64	42.7
	51	47.8	0.02	0.29	406	0.35	0.32	0.06	82	1.10	29.9
	52	46.9	0.02	0.21	411	0.30	0.25	0.07	69	1.17	30.9
	53	45.8	0.02	0.29	409	0.28	0.26	0.05	102	1.10	43.1
	54	44.8	0.02	0.40	415	0.44	0.31	0.05	91	1.42	34.3
	55	43.7	0.01	0.20	409	0.23	0.23	0.05	88	0.98	44.2
	56	42.2	0.01	0.13	413	0.19	0.07	0.07	67		48.5
	57	40.8	0.01	0.22	417	0.30	1.32	0.04	74	0.22	44.1
	58	40.0	0.02	0.24	411	0.29	0.38	0.06	81	0.77	24.4

Appendix: (Continued).

NP22	38	38.1	0.01	0.17	417	0.28	0.43	0.06	59	0.65	55.5
	37	36.9	0.04	0.95	417	0.79	1.00	0.04	119	0.79	41.2
	36	36.1	0.03	0.42	402	0.46	1.64	0.07	90	0.28	29.5
	35	35.5	0.01	0.20	410	0.28	0.28	0.05	71	0.99	72.4
	34	34.4	0.03	0.62	417	0.58	1.00	0.05	106	0.58	42.2
	33	33.3	0.02	0.44	408	0.42	0.95	0.04	105	0.44	44.9
	32	32.1	0.02	0.56	419	0.52	0.69	0.03	109	0.75	58.5
	31	31.0	0.03	0.68	423	0.63	0.73	0.04	106	0.88	52.6
	30	30.1	0.03	0.72	420	0.54	0.76	0.03	132	0.72	60.9
	29	29.2	0.03	0.71	420	0.57	0.83	0.03	123	0.69	54.0
	28	28.2	0.02	0.45	421	0.51	0.38	0.03	88	1.33	62.6
	27	27.2	0.02	0.32	420	0.79	0.28	0.04	41		67.6
	26	26.5	0.03	0.91	421	0.68	0.82	0.03	135	0.82	52.8
	25	24.9	0.03	0.85	421	0.57	0.61	0.03	148	0.94	60.6
	24	24.1	0.03	1.17	424	0.72	0.85	0.03	162	0.85	45.6
	23	23.0	0.03	0.72	427	0.62	0.52	0.03	117	1.18	59.4
NP21	22	22.2	0.04	1.29	429	0.88	0.52	0.03	146	1.69	59.3
	21	21.9	0.03	0.99	427	0.80	0.65	0.03	124	1.23	47.8
	20	19.1	0.03	0.31	404	0.36	1.76	0.07	86	0.20	28.1
	19	17.5	0.06	2.34	423	1.10	1.45	0.02	213	0.75	52.4
	18	16.2	0.05	2.35	424	1.21	1.38	0.02	193	0.88	49.3
	17	15.3	0.07	3.36	421	1.43	1.39	0.02	235	1.02	53.0
	16	14.6	0.07	3.31	423	1.46	1.30	0.02	226	1.12	51.5
	15	13.3	0.08	3.09	422	1.42	1.53	0.03	218	0.93	51.6
	14	12.0	0.08	3.35	422	1.50	1.46	0.02	223	1.03	52.6
	13	11.1	0.09	3.98	420	1.64	1.44	0.02	242	1.14	51.7
	12	10.1	0.09	2.96	421	1.39	1.43	0.03	213	0.97	48.5
	11	9.5	0.09	2.98	418	1.29	1.47	0.03	230	0.88	47.3
	10	8.3	0.10	4.48	420	1.78	1.38	0.02	252	1.29	50.5
	9	7.9	0.06	2.13	422	1.65	1.47	0.03	129	1.12	48.9
	8	6.8	0.07	2.94	419	1.43	1.59	0.02	206	0.90	46.8
	7	5.8	0.08	2.50	422	1.36	1.59	0.03	184	0.85	41.3
	6	4.9	0.09	3.48	422	1.65	1.50	0.02	211	1.10	43.2
	5	4.1	0.09	3.10	421	1.66	1.44	0.03	187	1.15	38.6
	4	3.4	0.09	3.62	422	1.49	1.37	0.02	243	1.09	48.1
	3	2.6	0.08	3.67	423	2.04	1.67	0.02	180	1.22	47.0
	2	1.6	0.03	1.36	430	0.97	0.53	0.02	140	1.81	64.7
	1	0.5	0.05	1.88	426	1.10	1.10	0.03	170	1.00	59.3

Appendix: (Continued).

	Footwall Section										
NP23	78	6.5	0.02	0.14	413	0.25	0.07	0.10	55	3.71	25.7
	77	5.9	0.02	0.15	409	0.21	0.45	0.09	73	0.46	55.6
	76	5.4	0.02	0.22	407	0.27	0.40	0.07	78	0.68	41.9
	75	4.8	0.01	0.06	434	0.22	0.18	0.14	27	1.19	59.2
	74	4.1	0.01	0.06	411	0.21	0.08	0.08	26	2.56	61.7
	73	3.3	0.01	0.11	420	0.31	0.17	0.08	36	1.85	43.2
	72	2.5	0.01	0.19	419	0.18	0.10	0.05	104	1.83	59.5
	71	1.7	0.01	0.12	418	0.50	0.17	0.04	23	2.87	66.9

TOC - total organic carbon, S - sulfur, HI - hydrogen index, PI - production index, calc. equi. - calcite equivalent.